Electronic Supplementary Material (ESI) for Physical Chemistry Chemical Physics.

Supporting Information

Defect engineering, microstructural examination and improvement of ultrafast third harmonic generation in GaZnO nanostructures: A study of e-beam irradiation

Albin Antony[1], Poornesh P[1*], I.V Kityk[2], K Ozga[2], G.Myronchuk[3], Suresh D Kulkarni[4], Ganesh Sanjeev[5],Vikash Chandra Petwal[6], Jishnu Dwivedi[6],Vijay Pal Verma[6]

1Department of Physics, Manipal Institute of Technology, Manipal Academy of Higher Education, Manipal, Karnataka, 576104, INDIA

2Institute of Optoelectronics and Measuring Systems, Faculty of Electrical Engineering, Czestochowa University of Technology, Armii Krajowej 17, PL-42-201 Czestochowa, Poland

3Solid State Physics Department, Eastern European University, Voli 6, Luck, Ukraine

4Department of Atomic and Molecular Physics, Manipal Academy of Higher Education, Manipal, Karnataka, 576104, INDIA

5Department of Physics, Mangalore University, Mangalore, Karnataka, 574199, India

6Industrial Accelerator Section, PSIAD, Raja Ramanna Centre for Advanced Technology, Indore 452012, M.P., India*Corresponding author: poorneshp@gmail.com, poornesh.p@manipal.edu (Poornesh P)

The supporting information details the nanostructure synthesis parameters and electron beam treatment procedures (Table S1 and S2). The optical properties studied using UV visible spectrometer is shown Fig S1 and S2. The detailed investigation on microstructural properties were shown in Table S3 and S4

2. Experimental procedures

2.1 Materials synthesis

Table S1. The experimental parameters followed for the growth of the GaZnO nanostructures

Experimental Parameters	
Substrate temperature	400^0C
Precursor concentration	0.05M
Ga doping concentration	3 Wt%
Solution flow rate	2 ml/min
Solution flow factor	1
Working pressure	1.5 bar
Distance between spray head and substrate	28cm

2.2 Electron beam Irradiation

The linear accelerator generates pulses at 300Hz each with a duration of 10μs. The electron beam generating system consist of a scanning magnet and trapezoidal shape scanning horn used to scan throughout the specimen using the electron beam. The scanning horn is attached with a titanium foil of 50μm thickness for transmitting the electrons from vacuum to atmosphere.

Table S2. Electron beam irradiation experiment parameters

LINAC Accelerator Experimental Parameters	
Beam energy	8MeV
Energy spread	0.35%
Beam current (pulsed)	50mA (max)
Pulse repetition rate	300Hz (max)
Average beam power	250W (max)
Pulse width	10μs (max)
Magnetic field strength	1927.5G
Magnetic power	2MW
Operating frequency	2998MHz
Dose rate at 1m	1 kGy/min
Distance from source to sample	30cm
Temperature during irradiation	Room temp.

Optical studies:

The absorption coefficient and Tauc plot analysis of pristine and EBI GaZnO are presented in Fig S1 and Fig S2. The absorption coefficient (Fig 1) shows a consistent increase upon increase in electron beam dosage possibly due to the dense distribution of grains without well-defined grain boundaries which further results in increase of shallow defect centres. Upon electron irradiation, the structure of the crystalline is same but a decrease in size may be observed i.e during electron irradiation there is a possibility of heat generation at the surface and this will produce the splitting of particles and due to tendency, the particles again reunite to form the original shape. During this period, the agglomerated or un-agglomerated particle creates shallow defects. The creation of shallow defect centres in the forbidden gap further resulted in the decrement of band gap as observed in fig 2. The variation in the surface morphology was detailed by atomic force microscopy (AFM) and shown in section 3.3

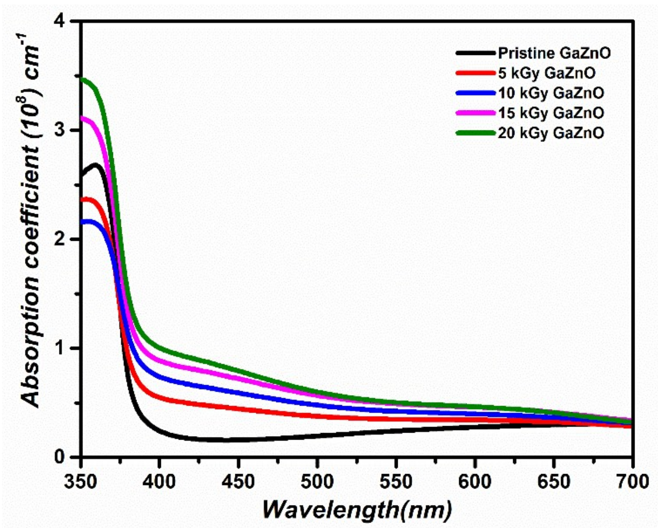

Fig S1. Absorption coefficient of Pristine and EBI GaZnO nanostructures

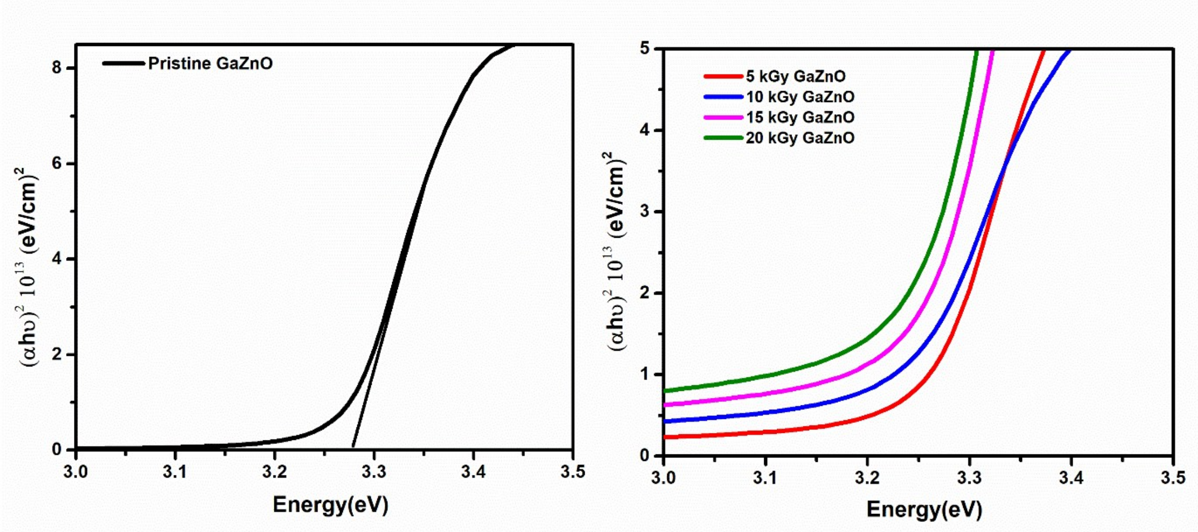

Fig S2. Tauc Plot analysis of pristine and EBI GaZnO nanostructures

Ultrafast nonlinear optical studies

The effect of photoinduction with a coherent CW laser light on the level of the third harmonic generation signal was examined. THG measurements were carried out before and after photoinduction. Photoinduced radiation was carried out up to 60 seconds. As a source of photoinduced radiation a continuous wave laser with radiation at 532 nm was used, while as a source of fundamental radiation a 10-nanosecond pulsed laser Nd: YAG with a wavelength at 1064 nm with frequency repetition 10 Hz was used. The power of the incident fundamental laser wavelength at 1064 nm was tuned by Glan's polarizer with laser damage power density 4 GW/cm^2. The laser beam profile diameter was equal to a about 8 mm. The maximum of the energy density was about 200 J/m^2. The femtosecond laser studies have been performed using the same set-up with replacing of the nanosecond lasers by the 120 fs lasers at 1045 nm laser with pulse energy varying up to 29 nJ. The value of fundamental laser energy signal was evaluated by the germanium photodetector and its third harmonic signal by a Hamamatsu photomultiplier with an installed interferometer filter at 355 nm with spectral width about 5 nm which transmits electromagnetic radiation with a wavelength at 355 nm. The maximal THG signal was detected by manual rotation of the samples in the 3 axis by observation of the maximal THG. Levels of obtained fundamental and third harmonic signals were measured using a Tektronix MSO 3054 oscilloscope with sampling of 2.5 GS. The oscilloscope and the rotary table digit signals were input to the two channels of the oscilloscope connected with PC. The entire measuring stand was placed under the box eliminating the influence of external undesirable light scattering.

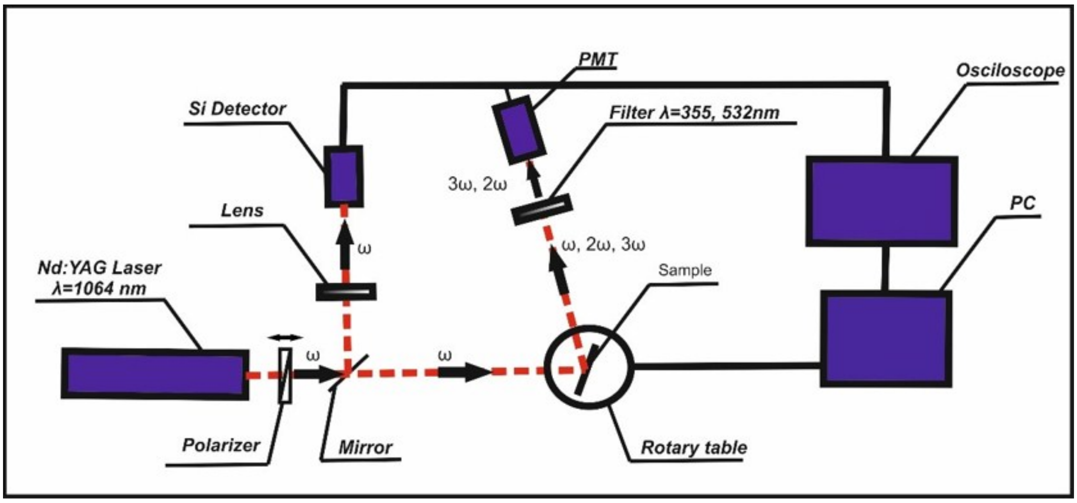

Fig S3 Schematic of experimental set up used for THG measurement

3. Result and discussion

3.1.1 Glancing angle x-ray diffraction studies (GXRD)

The values of inter-planner spacing (d-value) calculated from GXRD data indicates that d-value shows a non-monotonous variation. This observation can be explained on the basis of distortion of the crystal lattice. The distortion of the GaZnO lattice, arising from the variation of bond lengths and bond angles between atoms, develops the lattice strain. If the interplanar spacing of the plane changes it indicates the shifting of Bragg angle. Hence, the tensile stress increases the d-spacing which causes a shifting of peak towards lower 2θ values whereas compression stress decreases the d-spacing which results the shifting of peaks towards higher 2θ values. The analysis on GaZnO nanostructures thus confirms that EBI treatment at 20 kGy dosage results in a compressive stress resulting in the decrement of interplanar spacing along all crystallographic planes.

Table S3 Interplanar spacing (dexp) from XRD, JCPDS data card for corresponding hkl planes, percentage of variation of d

Pristine GaZnO nanostructures			
(hkl)	**d_{exp}(A^o)**	**d_{JCPDS}(A^0)**	**% of contraction in d**
100	2.810	2.813	0.1067
002	2.590	2.602	0.4611
101	2.470	2.475	0.2020
102	1.904	1.910	0.3141

110	1.622	1.624	0.1231
103	1.471	1.470	-0.0680

5 kGy GaZnO nanostructures			
(hkl)	**d_{exp}(A^o)**	**d_{JCPDS}(A^0)**	**% of contraction in d**
100	2.802	2.813	0.3910
002	2.593	2.602	0.3458
101	2.465	2.475	0.4040
102	1.903	1.910	0.3664
110	1.618	1.624	0.3694
103	1.471	1.470	-0.0680

10 kGy GaZnO nanostructures			
(hkl)	**d_{exp}(A^o)**	**d_{JCPDS}(A^0)**	**% of contraction in d**
100	2.821	2.813	-0.2843
002	2.596	2.602	0.2305
101	2.479	2.475	-0.1616
102	1.910	1.910	-
110	1.629	1.624	-0.3079
103	1.475	1.470	-0.3401

15 kGy GaZnO nanostructures			
(hkl)	**d_{exp}(A^o)**	**d_{JCPDS}(A^0)**	**% of contraction in d**
100	2.809	2.813	0.1421
002	2.601	2.602	0.0384
101	2.471	2.475	0.1616
102	1.908	1.910	0.1047
110	1.622	1.624	0.1231
103	1.475	1.470	-0.3401

20 kGy GaZnO nanostructures

(hkl)	**d_{exp}(A^o)**	**d_{JCPDS}(A^0)**	**% of contraction in d**
100	2.818	2.813	-0.1778
002	2.604	2.602	-0.0768
101	2.479	2.475	-0.1616
102	1.912	1.910	-0.1047
110	1.627	1.624	-0.1847
103	1.478	1.470	-0.5442

EBI Dosage (kGy)	**% of variation of Interplanar spacing 'd'**					
	(100)	**(002)**	**(101)**	**(102)**	**(110)**	**(103)**
Pristine	**0.1067**	**0.4611**	**0.2020**	**0.3141**	**0.1231**	**-0.0680**
5	**0.3910**	**0.3458**	**0.4040**	**0.3664**	**0.3694**	**-0.0680**
10	**-0.2843**	**0.2305**	**-0.1616**	**-**	**-0.3079**	**-0.3401**
15	**0.1421**	**0.0384**	**0.1616**	**0.1047**	**0.1231**	**-0.3401**
20	**-0.1778**	**-0.0768**	**-0.1616**	**-0.1047**	**-0.1847**	**-0.5442**

Table S4 Percentage variation in d upon EBI